Investigating Multi-Pulse Laser Wakefield Acceleration Through Simulations

Buddy William Alcock

Supervisor: Dr. Chris Murphy

Abstract

The aim of this project was to use simulations to design a particle accelerator based on laser-plasma interactions, where plasma waves are generated by laser pulses resulting in large accelerating fields. Specifically, this project will investigate the use of multiple lower energy laser pulses instead of a more conventional high energy single pulse system. It was seen that the suggested spacing from literature for the laser pulses was ineffective in the non-linear regime and had to be corrected for the relativistic masses of electrons. A system of five 0.15 J pulses, with the corrected spacing, achieved a maximum accelerating field of (406 ± 1) GV/m, in comparison a single 0.75 J pulse had an accelerating field of (422 ± 1) GV/m. The final pulse of the five laser pulse system was ineffective due to self-injection of electrons being achieved after the fourth laser pulse, producing electrons with a peak energy of (56.8 ± 0.1) MeV. The multi-pulse system achieved injection using 0.15 J less energy, demonstrating that multi-pulse could be a more efficient approach to laser wakefield acceleration going forward.

Department of Physics
University of York
YO10 5DD, UK
2024

Acknowledgements

I would like to acknowledge Professor Simon Hooker and his paper on multi-pulse laser wakefield acceleration, as his excellent paper steered the project in this direction. I would also like to thank my supervisor Dr Chris Murphy for his feedback and guidance, as well as for helping me to become a better physicist. Thanks to everyone and anyone who supported me along the way - I needed it.

Contents

1 Introduction

A plasma is typically a "fully or partially ionized gas consisting of electrons and ions" [1] and is often referred to as the fourth state of matter. Plasma can be generated by heating a neutral gas, compressing the gas or via energetic beams (such as beams of electrons or photons) [2]. Plasma can be used for a wide range of applications such as plasma surface modification, plasma cutters and nuclear fusion [3]. In this project it will be investigated how laser-plasma interactions can result in the acceleration of electrons up to relativistic velocities, using laser wakefield acceleration (LWFA).

In LWFA a laser pulse excites an electrostatic wake due to electrons being expelled by the ponderomotive force of a laser pulse [4] [5]. The ponderomotive force then generates large amplitude plasma waves (wakefields) [6] due to the restoring field from the charge separation of expelled electrons, this is known as the blow-out regime [7] [8]. Acceleration of particles occurs when they are injected, or self-injected, into the wakefield's accelerating electric field [9] [10]. Particles can also be injected across the wakefield (known as the surfatron regime) [11]. These injected particles can be accelerated up relativistic velocities on a millimetre scale [12].

Many designs for LWFA particle accelerators utilise a single high intensity laser pulse to drive wakefields, requiring lasers with energies around 5 J [13]. Lasers of this energy and of intensities of order 10^{18} W/cm^2 require large systems, large amounts of money. To reduce the cost and size of plasma accelerators, it has been suggested that a train of lower energy laser pulses could be used to excite plasma waves [14]. Using this multi-pulse system causes excitations to add coherently and can generate electron beams with energy on the GeV scale [14]. Plasma wakefields can be excited by multiple pulses if they are spaced temporally by T_{pe} [14] which is the plasma wave period,

$$T_{pe} = \frac{2\pi}{\omega_{pe}} [14] \tag{1}$$

Where ω_{pe} is the frequency of the plasma wave, known as the plasma frequency, given by

$$\omega_{pe} = \sqrt{\frac{n_e e^2}{m_e \varepsilon_0}} [15] \tag{2}$$

Where n_e is the number density of electrons in the plasma, m_e is the electron mass, e is the electron charge and ϵ_0 is the permittivity of free space. The most prominent paper on multi-pulse laser wakefield acceleration (MP-LWFA) is the work of Hooker et al "Multi-pulse laser wakefield acceleration: a new route to efficient, high-repetition-rate plasma accelerators and high flux radiation sources" [14], however Dr Hooker focuses mainly on the electric field generated by the system and the laser systems that are required for the multi-pulse scheme. Here the self injection [16] of electrons into the wakefields accelerating field will also be investigated.

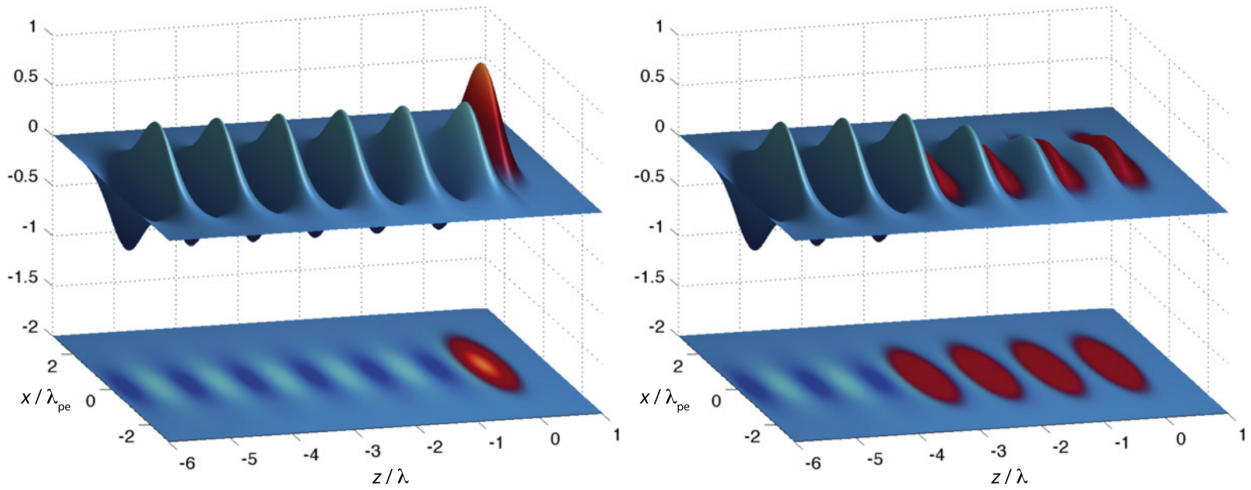

Figure 1: Comparison of a single pulse (left) and a multi pulse system (right), the blue is the electron density ($\frac{\Delta n_e}{ne}$) where $n_e$is the mean electron density)and the red is the laser intensity. The laser pulses propagate along z. Figure taken from *Multi-pulse laser wakefield acceleration: A new route to efficient, high-repetition-rate plasma accelerators and high flux radiation sources* [14].

In this project a single higher energy pulse will be compared with a train of five lower energy pulses, to investigate if a higher accelerating field can be generated using less energy. This is illustrated in figure 1, where it is shown that multiple laser pulses can produce the same wakefield as a single high energy pulse. The figure also shows that the lasers are spaced one plasma wave period apart.

If successful, a multi-pulse system would make particle acceleration more accessible to the scientific community, by reducing the energy requirements for laser wakefield acceleration. Plasma accelerators have broad applications including high energy physics, medical applications such as X-ray generation [17] as well as being used in electron microscopes [18].

2 EPOCH and the simulation

The simulations of the laser-plasma interaction are run using the software EPOCH, which is a particle in cell code (PIC) that is ran using Linux. PIC is a method where particles such as ions and electrons are grouped using a smaller number of pseudo-particles to reduce computational strain. EPOCH uses the finite-difference time-domain method to solve Maxwell's equations, calculating the fields, then solving the Lorentz force equation to calculate the force on the particles [19], this is shown in figure 2.
The finite-difference method is a numerical method for solving Maxwell's equations, for example

$$\left(\frac{\partial E_y}{\partial x}\right)_{i,j,k} = \frac{E_{y_{i+1,j,k}} - E_{y_{i,j,k}}}{\Delta x} \text{[19]} \tag{3}$$

where Δx is the distance between cells and E is the electric field.

A particle-in-cell method is used over the alternative methods (such as continuum methods or fluid models) as they can require a more complex numerical treatment which results in a more complicated code and longer simulation time. Other methods also have poor parallelisation compared to PIC, so they take longer to simulate. There is good agreement between PIC methods and grid based continuum methods [20], but PIC has been chosen for its simpler code and faster simulation time. A containerised version of EPOCH has been used to be more resource efficient, containerization is the packaging of the software with only the libraries needed to create a single executable that is lightweight [21]. A full compilation from source code was also used to access the Python libraries included in EPOCH.

EPOCH simulations use input files called input decks to specify the simulation conditions. Input decks consist of blocks that give EPOCH information about the size of the simulation, the properties of the laser pulse, the electron

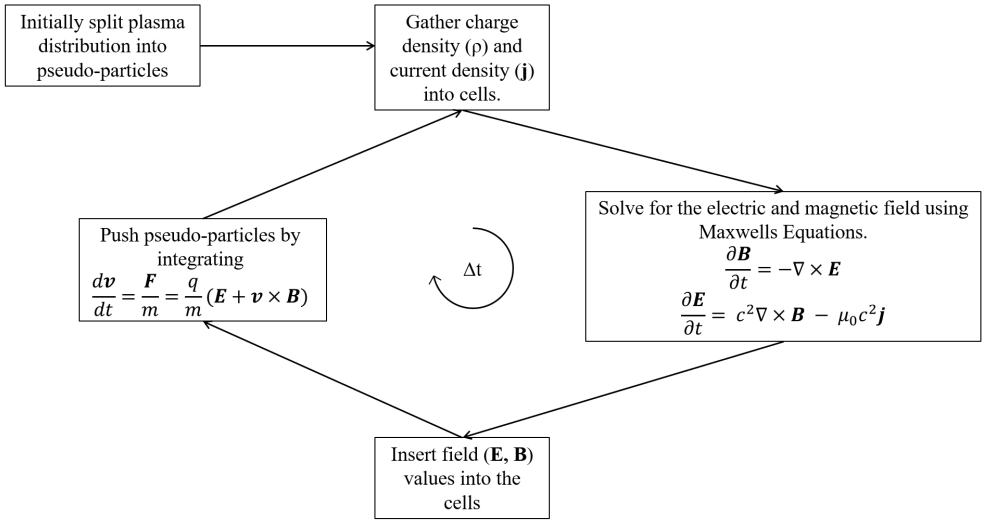

Figure 2: Diagram of how a particle-in-cell simulation runs and how the pseudo-particles are moved around according to the fields being generated, all steps are done for a small time step Δt. Steps taken from *Contemporary particle-in-cell approach to laser-plasma modelling* [19]

density, the simulation window, the outputted data, etc [22]. All simulations will be done using a moving window, where particles are removed on the on the left edge and new particles are introduced at the right edge. This helps to reduce the computational strain as particles that are not being accelerated exit the simulation window. In this window the plasma has a distribution that is supergaussian pointing in the y direction. This density distribution is to ensure that the simulation does not suffer from "edge effects" where the simulation boundaries cause nonphysical effects. The supergaussian prevents an increase in simulation time by allowing the simulation box to be increased in size, whilst keeping the amount of electrons being simulated the same. The window used in this simulation was 90μm in the x direction and 80μm in the y direction.

The physical system being simulated in this project is a gas jet being impinged on by a laser firing in a perpendicular direction to the gas jet. The laser beam then generates the laser wakefield as described earlier. The EPOCH simulation window described captures the laser beam(s) impinging on the plasma and then the resulting wakefield, the window is travelling in the same direction as the laser beam and is travelling at close to the speed of light. The simulation had to be slowed slightly to 99% of the speed of light, as the laser is travelling at the group velocity of the laser which is slightly slower than c. The physical system and simulation window is illustrated simply in figure 3.

3 Convergence testing

Convergence testing is performed by altering certain simulation properties to ensure that simulations are accurate. In this project convergence testing was performed for both the number of particles per cells and the number of cells per wavelength. By performing the same simulation with variations on these properties independently it should be seen that the simulation will begin to converge. In this case it has been chosen to examine if the maximum value of electric field is converged upon. This convergence testing will allow the uncertainty of the simulations to be quantified.

3.1 Particles per cell

To determine the uncertainty in the values produced from the simulation, the number of particles being simulated needs to be taken into account. In an EPOCH simulation the number of particles per cell can be set in the input deck, this value determines the number of pseudo-particles. A pseudo-particle represents a larger number of real particles (electrons), keeping the simulation less demanding. A larger number of pseudo-particles means more pseudo-particles to describe the movement of electrons being simulated. Simulating larger numbers of pseudo-particles results in longer simulation times but they are more accurate. To find the optimal number of particles per cell convergence testing was performed where the same simulation was ran multiple times with increasing values of particles per cell, ranging from

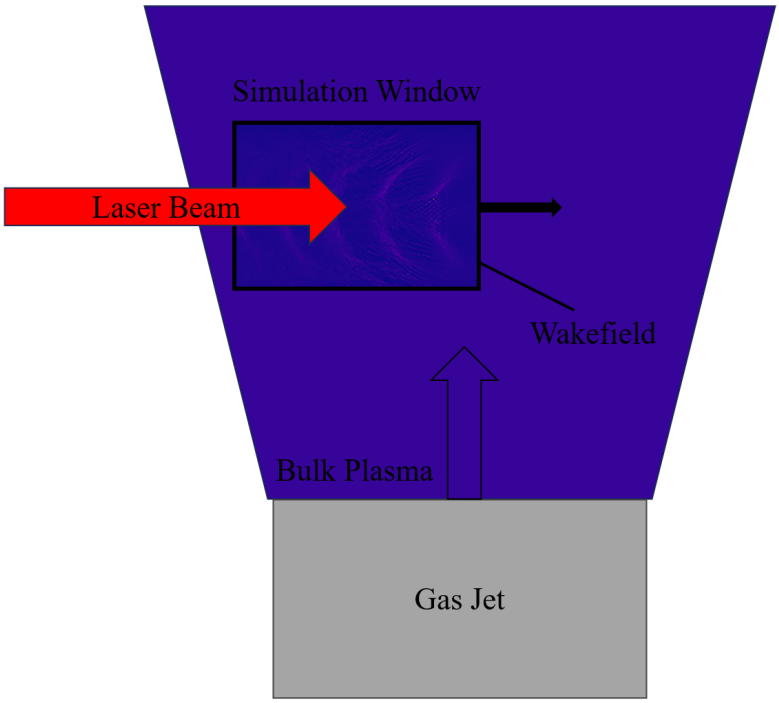

Figure 3: Simple illustration of the real system that is being simulated using epoch, a plasma jet (flowing upwards in this diagram) is impinged upon by a laser beam. The EPOCH simulation window simulates the laser and the resulting wakefield.

2 to 32 particles per cell.

Increasing the number of particles per cells resulted in a converged value of maximum electric field, given by the offset of the exponential decay that is fitted to the data - seen in figure 4. This value was $(6.48 \pm 0.007) \times 10^{10}$ V/m. It was decided that a value of 10 particles per cell would be used for the simulations in this project as that value resulted in a 0.120% deviation from the converged value of the maximum electric field. A larger value could have been chosen that was closer to the converged value, for example 24 particles per cell, but that would result in a longer simulation time. A simulation consisting of 32 particles per cell took $\sim$ 20 hours whereas a simulation of 10 particles per cell took $\sim$ 10 hours.

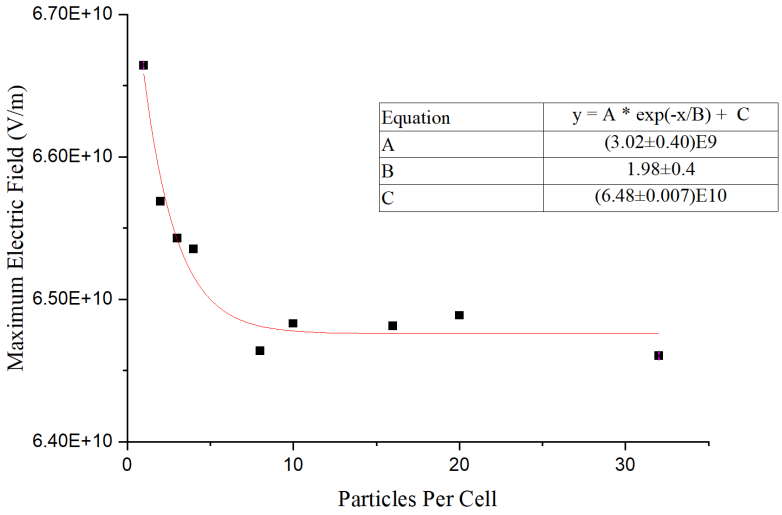

Figure 4: Plot of maximum electric field value against particles per cell at 3 ps. Data from an EPOCH simulation of a five pulse acceleration with a laser wavelength of 800nm and a laser energy of 0.5J. Data points seen in black with an asymptotic fit seen in red

3.2 Number of cells

The simulation window is split into a number of cells in x and y. The number of cells in the simulation window need to be accounted for in convergence testing. The larger the number of cells the larger number of pseudo-particles being simulated, due to the pseudo-particles being set as a number per cell. To quantify the number of cells being simulated, the width of the simulation window was divided by the wavelength of the driving laser. This total value was then multiplied by a value n which was the number of cells per wavelength - giving the number of cells to simulate. This is shown in equation 4.

$$N_{cells} = n \times \frac{w}{\lambda_L} \tag{4}$$

N_{cells} is the number of cells in x or y, n is the number of cells per wavelength, w is the width of the simulation simulation window in x or y and λ_L is the laser wavelength. A series of simulations were done at a value of 10 particles per cell with varying number of cells per wavelength, from 8 to 50 cells per wavelength.

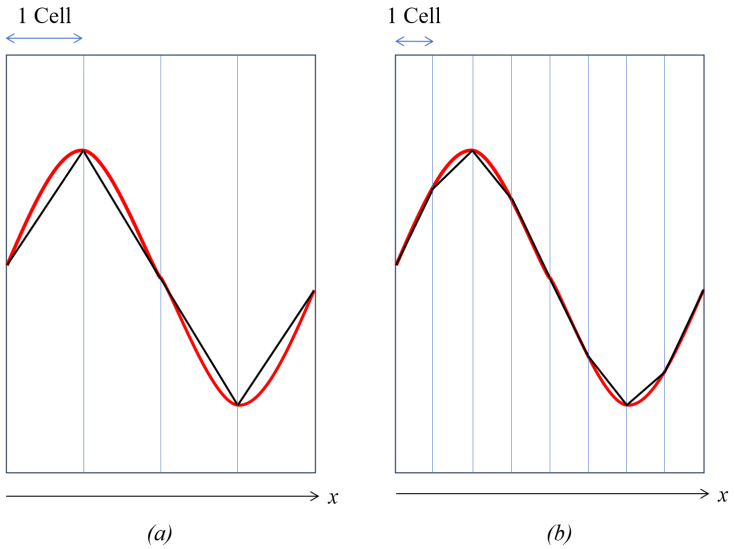

Figure 5: Diagram of how EPOCH resolves a lasers wavelength, in one direction, using the particle in cell method, the wavelength is in red, cell boundaries in blue and the resolved wavelength in bold black lines. (b) has a larger number of cells per wavelength and has a resolved wavelength much closer to the true wavelength.

If a low number of cells per wavelength is used then EPOCH resolves the wave very coarsely and does not capture the small changes in the lasers electric field (for example), with an increased number of cells per wavelength the wavelength is resolved more accurately - illustrated in figure 5. If a low number of cells per wavelength is used then the lasers can behave nonphysically, such as not propagating at the speed of light. Due to these factors having more cells per wavelength generates more accurate simulation results as the lasers are resolved properly and there are more pseudo-particles being simulated.

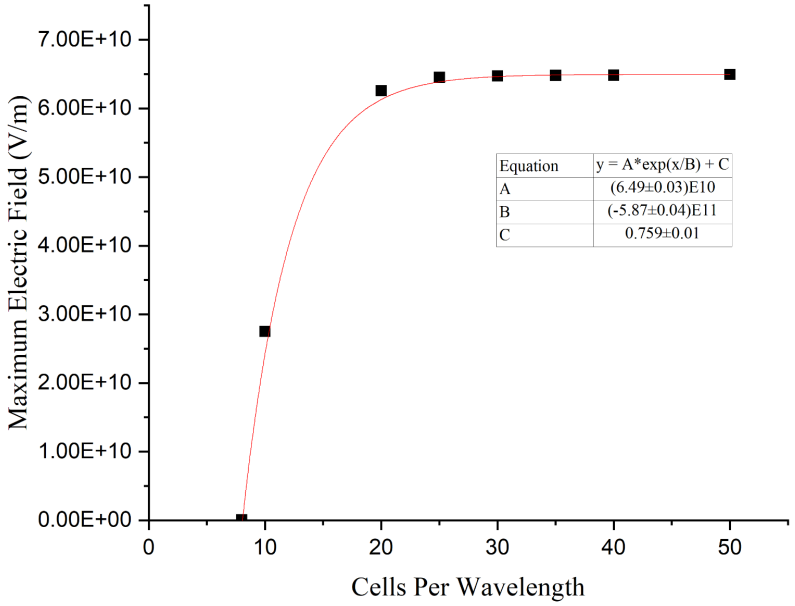

Figure 6: Plot of maximum electric field value against cells per wavelength at 3 ps. Data from an EPOCH simulation of a five pulse acceleration with a laser wavelength of 800nm and a laser energy of 0.5J. Data points seen in black with an asymptotic fit seen in red

For the number of cells per wavelength the value of maximum electric field converges at $(6.49 \pm 0.003) \times 10^{10}$ V/m which is within error range of the converged value for particles per cell, figure 5. A value of 30 cells per wavelength

was selected as being suitable as that resulted in a 0.2% deviation from the converged value with an acceptable simulation length. This value of 30 cells per wavelength equated to 3375 cells in the x direction and 3000 cells in y.

To quantify the total uncertainty in the simulation from the particles per cell and cells per wavelength, the square root of the sum of the uncertainties squared was taken. This resulted in a total uncertainty of 0.233%. It must be stated that this is not the total uncertainty of the simulation as this is a 2D simulation of a 3D system. A 3D simulation could not be performed as it would be too computationally intensive, so then it should be understood that while this is not a comprehensive analysis of all uncertainties it is the quantified uncertainties from the parameters set.

4 Multi-pulse

$$T_{pe} = \frac{2\pi}{\omega_{pe}} [14] \tag{1}$$

$$\omega_{pe} = \sqrt{\frac{n_e e^2}{m_e \varepsilon_0}} [15] \tag{2}$$

$$T_{pe} = \frac{\lambda_{pe}}{v_{pe}} \tag{5}$$

A plasma density of 1×10^{25} m^{-3} was used giving a plasma frequency of 1.81×10^{14} rad·s^{-1} from equation 2. This gives a plasma wave period of 34.8 fs which is the time spacing required between laser pulses to result in coherent addition. To verify this experimentally the wavelength of the wakefield can be measured and divided by the speed of the plasma wave (group velocity), this is shown in equation 5 where v_{pe} is the speed of the plasma wave. As the pulses separated by 34.8 fs in time, a pulse duration of 10 fs was used so that the pulses did not overlap with each other. This would be considered a cutting edge pulse duration as the Vulcan 20-20 upgrade at the Central Laser Facility in Oxfordshire aims to produce a laser of 500 J at 20 fs [23], so the lasers used in these simulations would be lasers that may be available in the near future.

A series of simulations will be performed where one, two, three, four and five pulses are simulated. The electric field at each time step will then be plotted and this will be compared for the different pulses, to demonstrate the increase in acceleration the electrons experience. Figures for the electric field and the momentum, energy and density of electrons will be produced by analysing the simulation data using Python and EPOCH Python libraries.

A higher energy single pulse simulation will also be performed to compare the single and multi-pulse approach and to determine if higher electric fields can be produced using multiple pulses while using the same amount of energy. It will also be concluded what the electric fields observed could be used for, if particles were injected into the system what velocities could they reach over a small scale ($\sim$ mm).

5 Self injection

If electrons have relativistic velocities then they are considered to be "self injected". This occurs when plasma waves reach high (wave-breaking) levels and background electrons are injected into the plasma waves [24]. Background electrons are injected when they have velocity approaching the phase velocity of the wakefield [25]. The energy or momentum distribution of the electrons can be used to determine if electrons have been self injected, as injected electrons will have much higher energies or momenta. A beam energy can be calculated if electrons are self injected, using equation 6.

$$E^2 = (pc)^2 + (m_0 c^2)^2 \tag{6}$$

E is the energy, p is the momentum, m_0 is the rest mass of the electron and c is the speed of light. The momentum distribution of both the single and multi-pulse system will be analysed to determine if any self injection has occurred, and if so what is the energy of the electron beam generated as well as what this electron beam could be used for.

6 Results and Discussion

6.1 Multiple pulses

6.1.1 Laser pulses and electric field

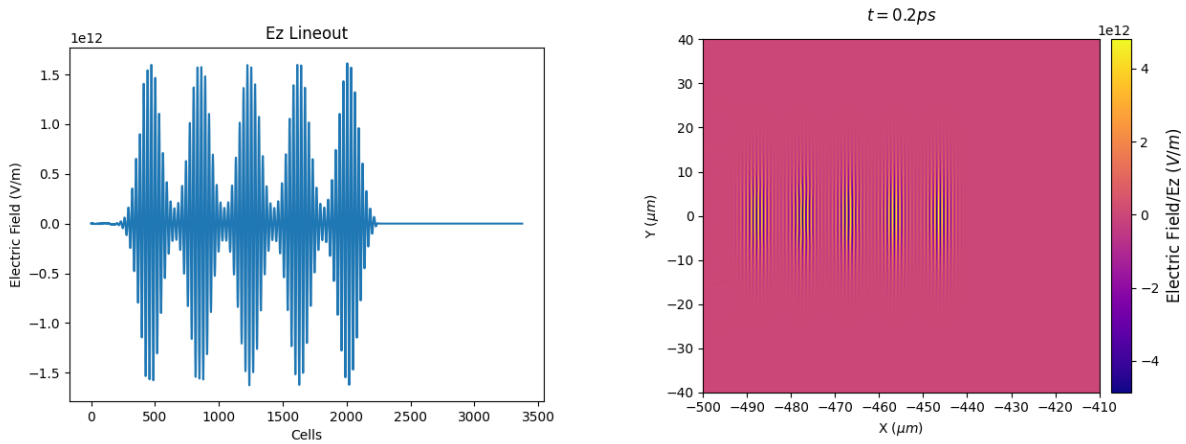

(a) (b)

Figure 7: (a) Line out of the z component of the electric field at 0.2 ps from the five pulse simulation, figure generated by plotting the electric field E_z at $y = 0$ using python. (b) Image of E_z at the same time step generated in Python using EPOCH libraries.

The multiple laser pulses used in the initial simulations were separated by $34.8fs$ which is a separation of 10μm in space as the lasers are travelling at the group velocity (slightly less than c). This separation can be verified in figure 7 (a), which is a figure of the line out of electric field component in the z direction. The lasers used in this simulation have all been polarised so that they are in the z plane, as this is a 2D simulation with particles only moving in x and y there is no other source of electric field in the z direction (E_z) apart from the lasers.

Figure 7 (a) was produced by extracting E_z data to a .csv file and then plotting the value of E_z at $y = 0$. The y axis is cells - this refers to the cells being simulated by EPOCH. As the total number of cells and how big the simulation box is in real space is known, it is more convenient to work in number of cells and convert that to real space, rather than relabelling axes ticks in Python which can cause inaccuracies.

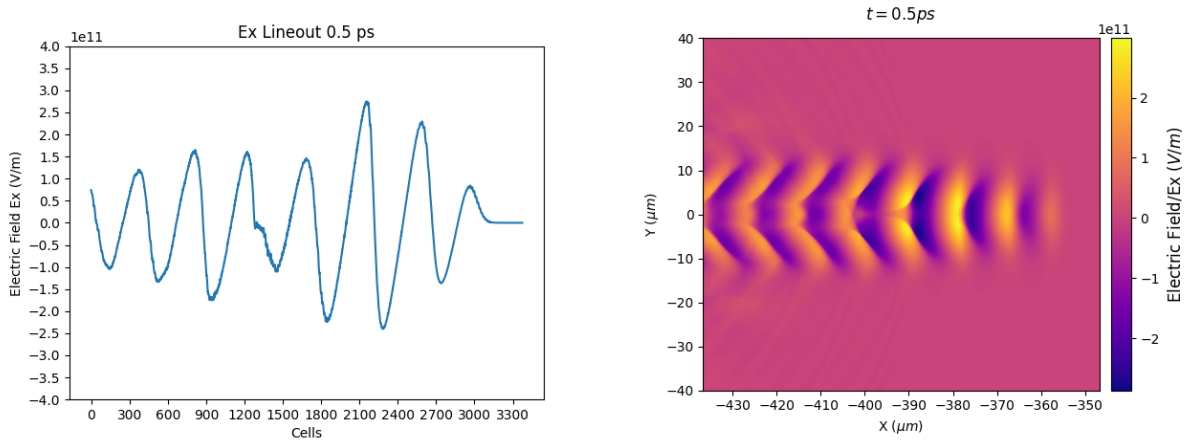

(a) (b)

Figure 8: (a) Line out of the electric field for a five pulse simulation at 0.15J for each pulse. (b) Figure generated from the same simulation and time using EPOCH library sdf helper.

The electric field generated by the five pulses can be seen in figure 8 (b), the brighter parts are areas of strong positive electric field and the darker areas are strong negative electric field. The line out, figure 8 (a), is the value of the electric field at $y = 0$ and more clearly illustrates the points of negative and positive electric field, as well as showing the wave form of the plasma wave. The maximum electric field was $(2.99 \pm 0.007) \times 10^{11}$ V/m, which was found by examining the array used to create the line out figure. However, the expected result is not seen - the accelerating electric field is not increasing with each pulse. This is could be due to the laser spacing being incorrect, and the fourth and fifth laser pulses are disrupting the wakefield. This is indicated in figures 9 and 10. In the centre of figure 9 (b) there is a reduction of electric field in the centre of the wakefield, which is less prevalent in the three pulse simulation seen in figure 9 (a).

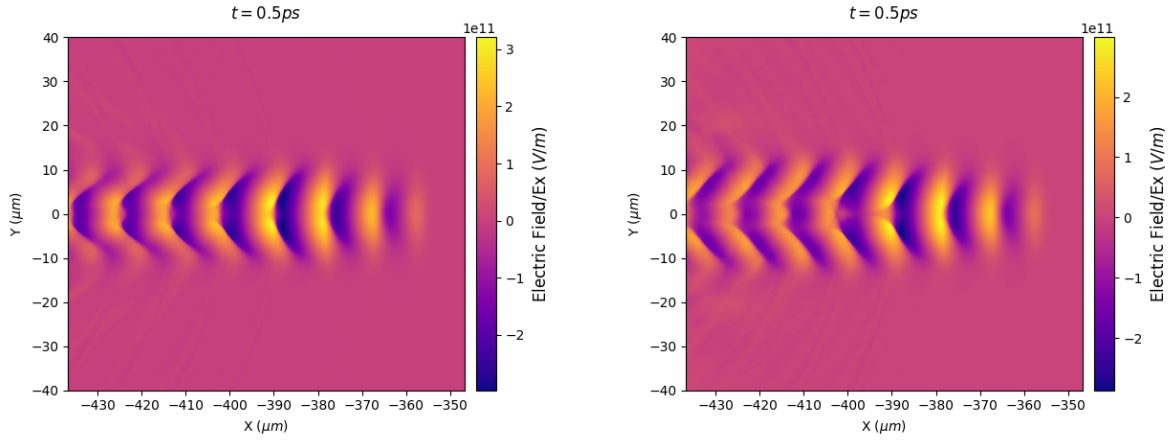

(a) (b)

Figure 9: (a) Electric field from the three pulse simulation at 0.5ps, generated from EPOCH library sdf helper. (b) Electric field from the five pulse simulation at 0.5ps.

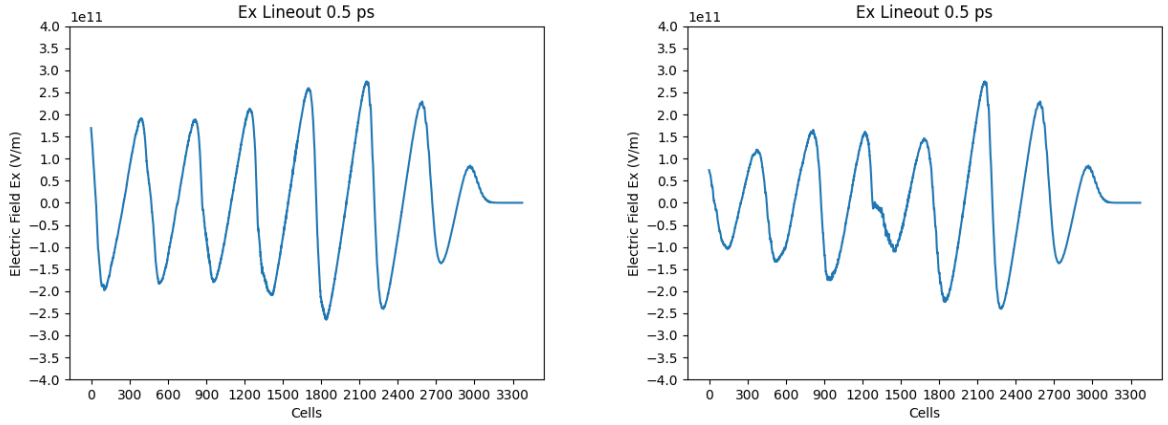

(a) (b)

Figure 10: (a) Electric field line out line out from three pulse simulation at 0.5ps with each pulse having energy 0.15J (b) Electric field from five pulse simulation at 0.5ps at 0.15J

The line out of the electric field, figure 10, makes it clearer that the laser is striking at the incorrect time. It can be seen in figure 10 (b) that the electric field is not growing with each pulse, as would be expected, and is instead weakening after the third pulse - evidence that the laser spacing for the fourth and fifth pulse is not ideal. In contrast the electric field in the three pulse simulation, figure 10 (a), grows after each pulse and tails off after that - as expected.

6.1.2 Electron density - the wakefield

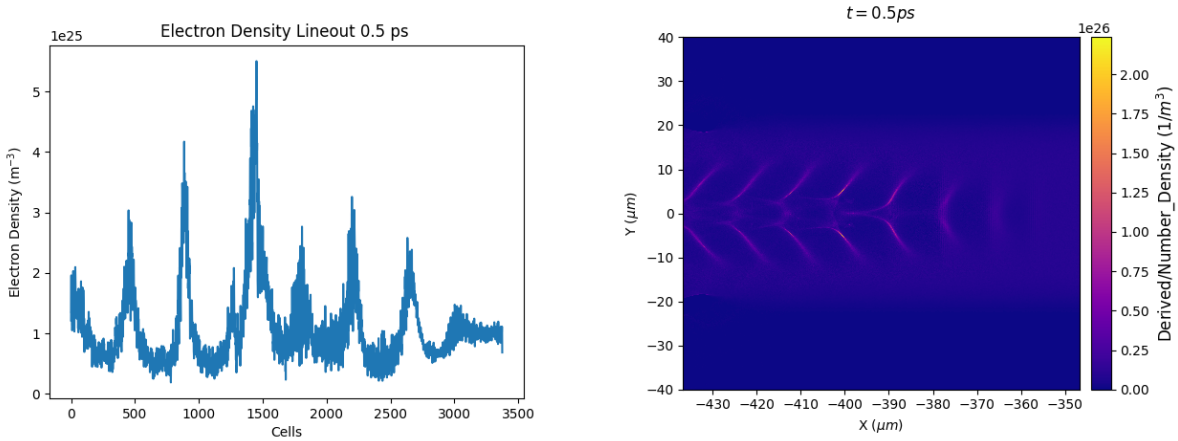

(a) (b)

Figure 11: (a) The line out of the electron density at 0.5 ps from the five pulse simulation where each pulse is 0.15J, this line out was performed in Python in the same way that the line out for the electric field was performed. (b) Figure generated by EPOCH library sdfhelper for the same simulation and time step as the line out was generated.

The wakefield generated by the five laser pulses can be seen clearly in figure 11 (b), the brighter lines in the figure indicate areas of higher electron density and clear wave structures can be seen. These areas of high electron densities are where electrons are being trapped by the potential wells of the wakefield. This can also be seen from the line out, figure 11 (a), which takes the density value at each cell at $y = 0$. The large spikes in the figure show that large amounts of electrons are being trapped periodically. In both figure 11 (a) and (b) it can be seen that there is a significant drop

in electron density at $-390\mu m$ or between 1500 and 1200 cells on the line out, this corresponds to the same point. If the electric field component in the z direction is analysed, figure 12, it can be seen that the centre of the fourth laser pulse is just after the $1800th$ cell in the simulation, this equates to -392μ m, which is where the disruption in electron density is. This is evidence that the laser spacing is incorrect, as the laser is disrupting the wakefield by firing directly into a bunch of trapped electrons therefore disrupting the wakefield.

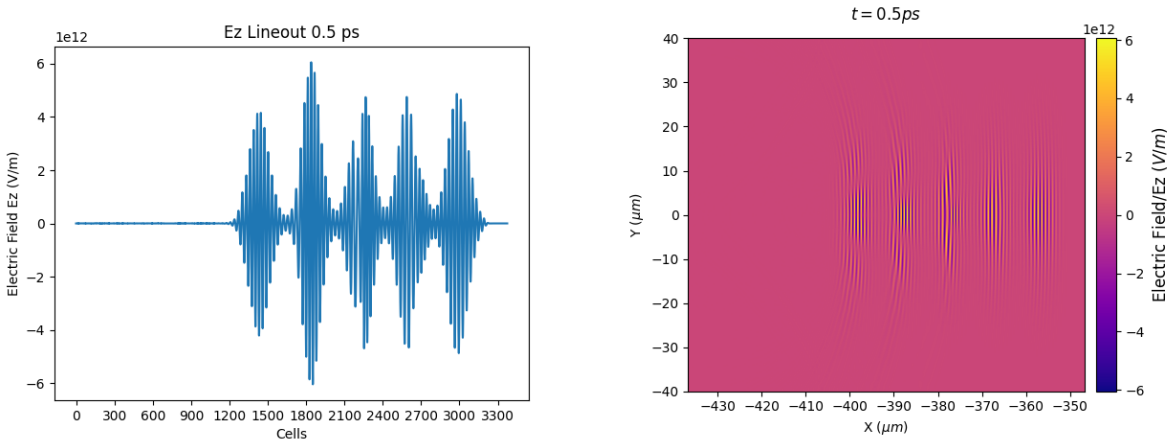

(a) (b)

Figure 12: (a) The line out of the E_z at 0.5 ps from the five pulse simulation where each pulse is 0.15J. (b) Figure generated by EPOCH library sdfhelper for the same simulation and time step as the line out was generated.

To determine the correct laser spacing the wavelength of the wakefield needs to be measured and the period of the plasma wave needs to be calculated, equation 5. The distance between the peaks of the x component of the electric field is the wavelength of the wakefield, and was measured from this data to be $(12\pm0.03)\mu$m. The wakefield is moving at the laser group velocity so the period is (40 ± 0.09) fs, larger than calculated using the same methods as Hooker et al in his paper on the multi-pulse regime [14]. An explanation for this is electrons having relativistic velocities and therefore having a relativistic mass. This is not widely discussed in his paper, he mentions that the wakefield generated by his pulse train is "mildly non-linear" and so they did not need to adjust the spacing for relativistic detuning [14]. In these simulations lasers of 0.15 J were used whereas he used lasers of 10 mJ, so the energy difference explains why the relativistic detuning occurred here whereas his simulation was only weakly affected by it at 200 pulses. The relativistic detuning can be quantified by the electron mass and its effect on the plasma frequency.

$$m_{rel} = \gamma \cdot m_e \tag{7}$$

$$\gamma = \frac{1}{\sqrt{1 - \frac{v_{pe}^2}{c^2}}} \tag{8}$$

$$\omega_{pe,rel} = \sqrt{\frac{n_e e^2}{\gamma m_e \varepsilon_0}} \tag{9}$$

The relativistic mass can be calculated by multiplying the electron mass by the Lorentz factor, equation 7, the Lorentz factor is given by equation 8 where v_{pe} is the plasma wave velocity. The relativistic mass effects the plasma frequency as seen in equation 9. To calculate the new spacing the distance between peaks in E_x was measured and converted into the time period which was calculated to be (40 ± 0.1) fs.

6.1.3 Laser spacing corrected for relativistic effects

Figure 13 indicates that the new spacing has improved the results drastically, the maximum electric field at 1 ps has nearly doubled. However, there are some abnormalities at the rear end of the simulation box which signals that there

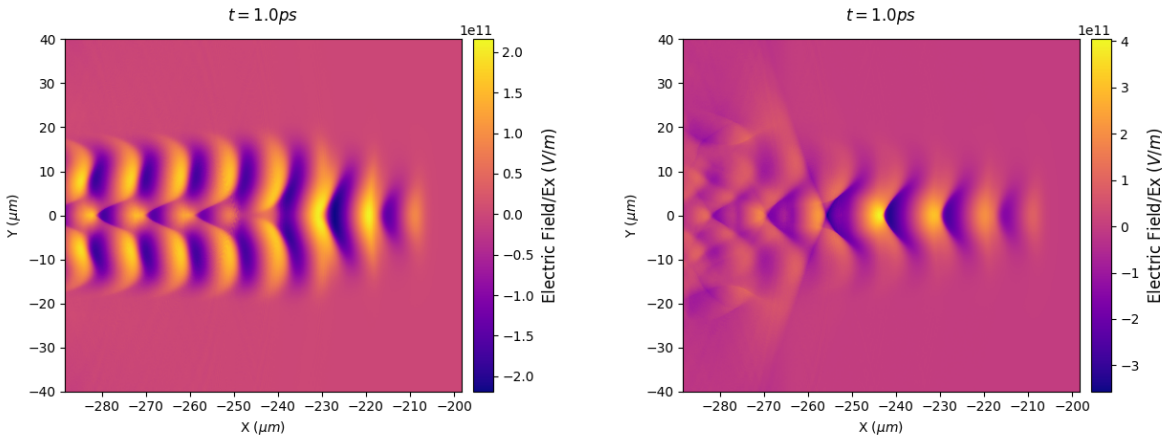

(a) (b)

Figure 13: (a) The electric field from the five pulse simulation where laser pulses are separated by 34.7 fs and lasers have energy of 0.15 J. (b) The electric field for five pulse simulation with the new spacing of 40 fs.

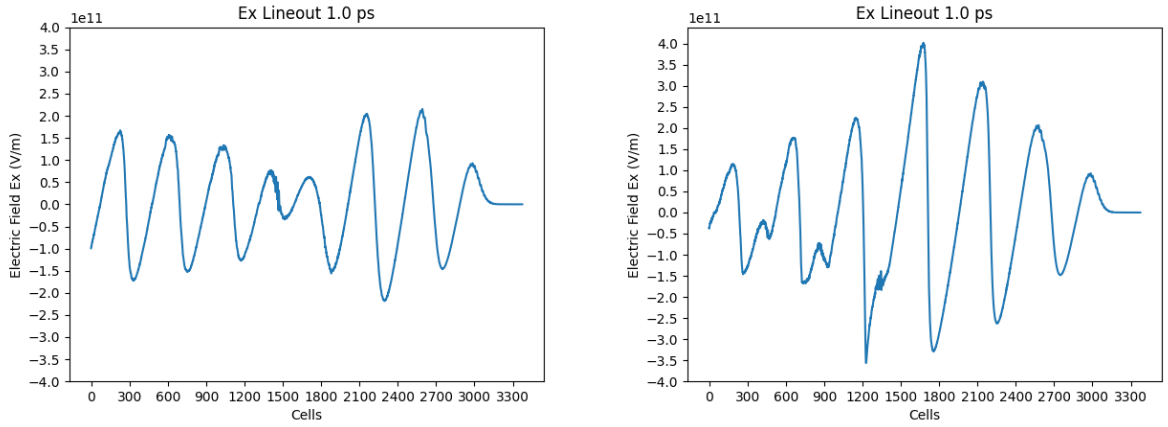

(a) (b)

Figure 14: (a) Line out of the electric field for the five pulse simulation with laser spacing of $34.7fs$. (b) Line out of the electric field for the five pulse simulation with laser spacing of $40fs$.

are still some issues with the laser spacing. This is seen more clearly in figure 14, where it can be that while the electric field grows for the first four pulses, it then reduces and there are some anomalies - dips and spikes here that would not be expected. From this simulation, it can be seen the first four pulses are spaced correctly but the fifth pulse is disrupting the wakefield. This is verified by examining E_z at 1 ps and seeing that the fifth pulse is striking at -260μm, or the 1200th cell, seen in figure 15, which is the point at which these defects occur in E_x.

It was initially thought that the last laser pulse needs a different spacing than the rest of them, this was again calculated by measuring the distance between peaks, in this case the distance between the third and fourth peak was measured to be $(14.5 \pm 0.03)\mu$m in space which is a time spacing of (48.3 ± 0.1) fs. Another multi-pulse simulation was ran with the final pulse having this larger spacing of (48.3 ± 0.1) fs and the other pulses having a spacing of (40 ± 0.1) fs.

Some improvements to the x component of the electric field were seen, particularly the reduction of spikes/dips towards the back of the simulation box, seen in figure 16. This suggests that the fifth laser was closer to its optimal position. The maximum of the electric field did not change significantly, the x component of the electric field peaked at (404 ± 1) GV/m. The wakefield has stabilised comparatively to the last simulation and the electric field does not drop as much after the fourth peak. Ideally a fifth peak would be seen as the electric field grows after the fifth laser pulse, but the

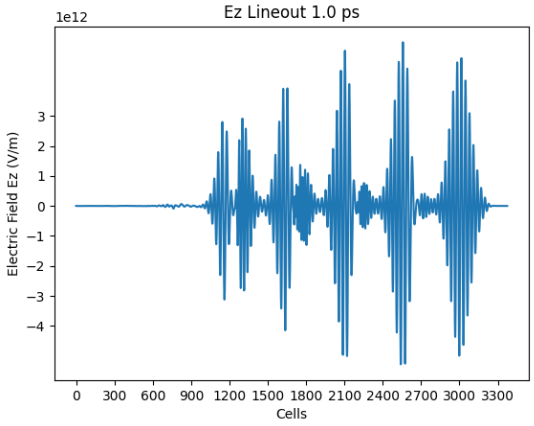

Figure 15: Line out of the electric field z component at 0.5 ps for a five pulse simulation at 0.15 J.

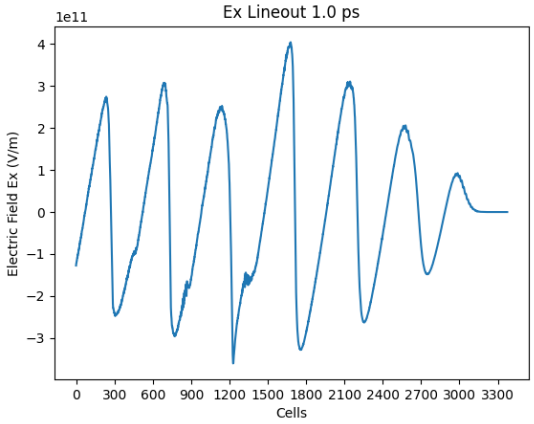

Figure 16: Line out of the electric field z component at 0.5 ps for a five pulse simulation at 0.15 J, first four pulses spaced at 40 fs with the last spaced at 48.3 fs.

spacing of that last pulse was not correct and did not allow for this.

6.1.4 Comparison with a single high energy pulse

Figure 17 (a) shows the wakefield generated by the single pulse system, with the area at the front of the box being the point at which the laser clears the electrons and the wakefield then follows. Figure 17 (b) shows the same for the multi-pulse system, the disruption caused by the fifth laser pulse can be seen in (b) between -260μm and -250μm.

Figures 18 (a) and (b) compare the electric field generated by the single and multi-pulse systems and it can be seen from the figures that they produce very similar accelerating fields in the x direction. The single pulse system reached a maximum of (422 ± 1) GV/m and the multi-pulse system achieves an electric field of (406 ± 1) GV/m. The multi-pulse system is thus less energy efficient in this scenario as it fails to generate a larger electric field. However, it has to be considered that the fifth pulse in this system is not as efficiently spaced as it could be.
Figures 19 (a) and (b) compare the derived average electron energy for the two systems at 1 ps. The bright spots indicate bunches of high energy electrons, again for the two systems the results are very similar, the single pulse system had a peak electron energy of $(9.75 \pm 0.02) \times 10^{-12}$ J at 1 ps and the multi-pulse system had a peak of $(9.08 \pm 0.02) \times 10^{-12}$ J, this is (60.9 ± 0.1) MeV and (56.8 ± 0.1) MeV respectively. The multi-pulse system achieves injection using just four pulses at $0.15J$ (0.6 J in total). The difference in energy of the injected electrons in the two systems is (4.1 ± 0.01) MeV, which is a small energy difference when taking into consideration that there was a difference of 0.15 J in the

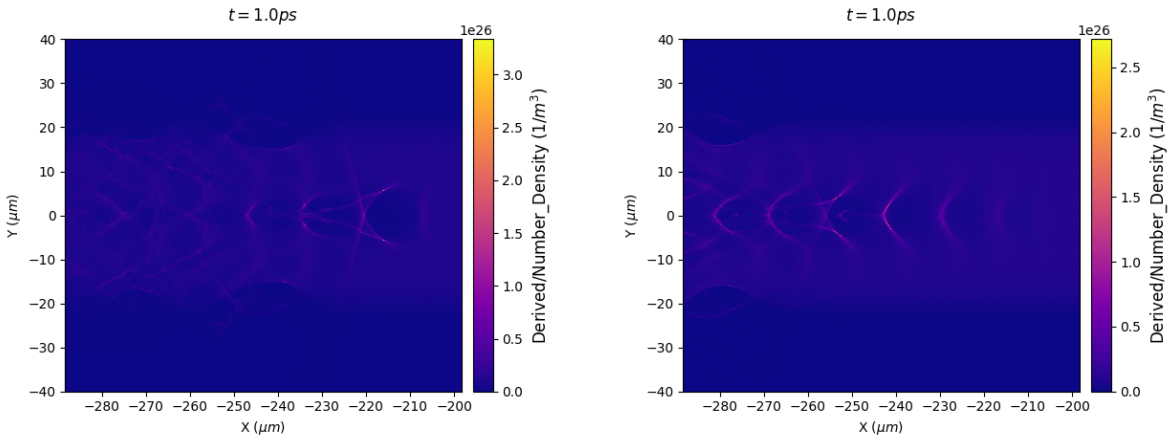

(a) (b)

Figure 17: Figures produced using Python and EPOCH library sdf helper. (a) Electron density for the single pulse simulation with a laser energy of 0.75J. (b) Electron density for the five pulse simulation with laser energy of 0.15J per pulse.

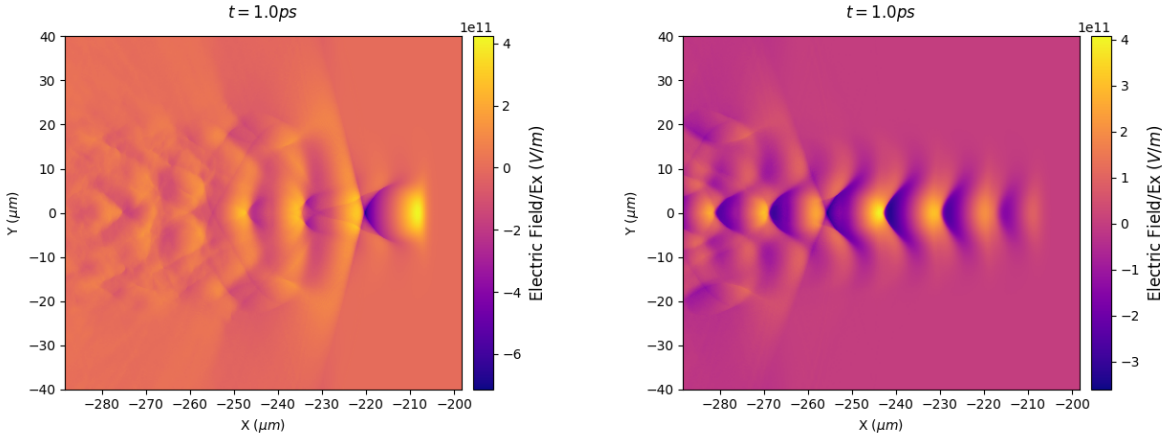

(a) (b)

Figure 18: Figures produced using Python and EPOCH library sdf helper. (a) x component of electric field for the single pulse simulation with a laser energy of 0.75J. (b) x component of electric field for the five pulse simulation with laser energy of 0.15J per pulse.

energy of the laser systems.

After seeing the injection in the multi-pulse systems it becomes clear that the fifth pulse is not misplaced, in terms of what was expected, but rather that the fifth pulse is ineffective due to injection already occurring. Injection happens after 250μm which is just after the fourth pulse. The fifth pulse fails to add to the wakefield after injection as the relativistic electrons generate a wakefield of there own in the background plasma - similar to wakefields generated in plasma wakefield acceleration (PWFA). In PWFA electrons are used to drive a wakefield instead of a laser [26], and the wakefield generated by the injected electrons interferes with the initial wakefield. It would be possible to space the last pulse so that the electric field would grow further, however it becomes non-trivial to calculate the new spacing caused by the interference of the two wakefields - requiring a longer project to fully investigate this.

Both systems underwent dephasing at later times in the simulation, where trapped electrons are moving faster than the accelerating wakefield. This occurs as the high energy electrons are travelling at $v_e \approx c$ whereas the wakefield is travelling at the group velocity of the plasma ($v_{wakefield} < c$) [27]. This leads to these energetic electrons moving

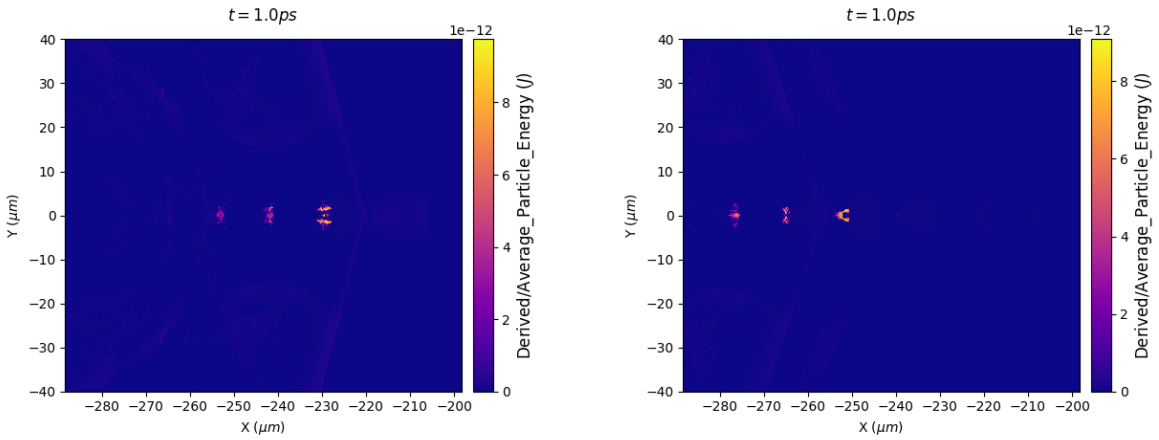

(a) (b)

Figure 19: Figures produced using Python and EPOCH library sdf helper. (a) Derived electron energy for the single pulse simulation with a laser energy of 0.75J. (b) Derived electron energy for the five pulse simulation with laser energy of 0.15J per pulse.

forward relative to the wakefield, dephasing, and entering a decelerating electric field region where they lose energy [28]. There are multiple approaches to limiting the dephasing effects, the simplest being to reduce the base plasma density. Reducing the density increases the dephasing length, L_d, as they have the relation $L_d \propto n^{-\frac{3}{2}}$ [29]. However reducing the plasma density increases the spacing of the laser pulses, which would mean a larger simulation window within which to fit them. Sadly this was not feasible for this project as the simulations would be much larger than the ones performed and take much longer to complete, but this would be an interesting direction to take this research.

The relativistic electrons produced by the multi-pulse system could be used for a few different purposes. This legitimises the research done as there are real applications for a system such as this. For example these electrons could be used to create a spectrum of x-rays by firing the electron beam at a metal target. They could also be used in inverse Compton scattering to produce high energy photons or, in medical physics, it has been proposed that electrons of order $10MeV$ can be used to treat skin cancer [30].

When comparing the multi-pulse and single pulse simulations it is evident, in this scenario, that the multi-pulse is more energy efficient as it achieves similar results, including self injection, while using less energy. This aligns with the main aim of this project, demonstrating that multi-pulse wakefield acceleration can be more energy efficient. Despite the results from this project it must still be considered that these are 2 dimensional simulations of what would be a 3 dimensional system in reality. There could be indeed be interactions in the plasma that are not accounted for here that should be examined further through physical experiments, before stating that multi-pulse laser wakefield acceleration is clearly more energy efficient.

7 Conclusion

A multi-pulse system with five pulses, at 0.15 J each, managed to achieve self-injection after just four pulses, producing an accelerating electric field in the x direction, E_x, of (406 ± 1) GV/m at 1 ps. The self-injected electrons from the multi-pulse system had a peak energy of $(9.08 \pm 0.02) \times 10^{-12}$ J or (56.8 ± 0.1) MeV. The effective energy to produce these results was 0.6 J as the final pulse was ineffective due to injection having already been achieved - disrupting the wakefield after the fifth pulse. In comparison, at 1 ps a single pulse of 0.75 J generated an electric field of (422 ± 1) GV/m and also achieved self-injection of electrons with peak energy of $(9.08 \pm 0.02) \times 10^{-12}$ J or (60.9 ± 0.1) MeV.

Based on these results it can be concluded that using multiple smaller energy laser pulses can be more efficient than a single high energy pulse. However, for an efficient system the spacing of the laser pulses differs in the linear and non-linear regimes, as the plasma frequency (and therefore plasma period) changes. Using the spacing suggested by

Hooker et al [14] for multi-pulse laser wakefield acceleration only holds for low energy laser pulses (of the order 10 mJ), but to achieve self injection higher energy pulses are required and this spacing does not account for the relativistic detuning. To design an efficient multi-pulse system the plasma wavelength must be measured, in the non-linear regime, from a preliminary simulation to calculate the plasma wave's period - which is the correct spacing for the laser pulses.

For future work, increasing the accelerating electric field with pulses after injection could be investigated by analysing the interference between the original wakefield and the wakefield generated by the injected electrons. Another direction could be to reduce the energy of the laser pulses, to utilise a greater number of pulses before injection occurs. The properties of currently available lasers could be used as a guideline for this work, such as an EKSPLA ultraflux laser that can deliver 50 mJ over 10 fs [31]. The dephasing in the system could also be investigated, which would entail lowering the density of the plasma. This lower density requires the laser pulse to be spaced further apart, requiring a larger simulation window and therefore longer simulations that were not possible here.

References

[1] A Piel. *Plasma Physics: An Introduction to Laboratory, Space, and Fusion Plasmas Second Edition*. Springer, 2017. P. 1-4, ISBN: 3319634259.

[2] H Conrads and M Schmidt. Plasma generation and plasma sources. *Plasma Sources Science and Technology*, 9:441, 10 2000.

[3] T Eastman. A survey of plasmas and their applications. *Plasma Physics Applied*, 2006.

[4] R. Assmann, R. Bingham, T. Bohl, and et al. Proton-driven plasma wakefield acceleration: A path to the future of high-energy particle physics. *Plasma Physics and Controlled Fusion*, 56(8), 2014.

[5] T. Tajima and J. M. Dawson. Laser electron accelerator. *Phys. Rev. Lett.*, 43:267–270, Jul 1979.

[6] E. Esarey, C. B. Schroeder, and W. P. Leemans. Physics of laser-driven plasma-based electron accelerators. *Rev. Mod. Phys.*, 81:1240, 2009.

[7] N. Barov, M. Conde, J.B. Rosenzweig, and et al. Measurements of plasma wake-fields in the blow-out regime. *Proceedings of the IEEE Particle Accelerator Conference*, 1:631 – 633, 1995.

[8] A. Golovanov, I. Yu. Kostyukov, A. Pukhov, and et al. Energy-conserving theory of the blowout regime of plasma wakefield. *Physical Review Letters*, 130(10), 2023.

[9] K.V. Lotov, A.P. Sosedkin, A.V. Petrenko, and et al. Electron trapping and acceleration by the plasma wakefield of a self-modulating proton beam. *Physics of Plasmas*, 21(12), 2014.

[10] J. Osterhoff, A. Popp, Zs. Major, and et al. Generation of stable, low-divergence electron beams by laser-wakefield acceleration in a steady-state-flow gas cell. *Phys. Rev. Lett.*, 101:085002, Aug 2008.

[11] T. Katsouleas and J.M. Dawson. A plasma wave accelerator – surfatron i. *IEEE Transactions on Nuclear Science*, 30(4):3241 – 3243, 1983.

[12] W.P. Leemans, B. Nagler, A.J. Gonsalves, and et al. Gev electron beams from a centimetre-scale accelerator. *Nature Physics*, 2(10):696 – 699, 2006.

[13] S.P.D Mangles, C.D. Murphy, Z. Najmudin, and et al. Monoenergetic beams of relativistic electrons from intense laser-plasma interactions. *Nature*, 431(7008):535 – 538, 2004.

[14] S.M. Hooker, R. Bartolini, and S.P.D. Mangles. Multi-pulse laser wakefield acceleration: A new route to efficient, high-repetition-rate plasma accelerators and high flux radiation sources. *Journal of Physics B: Atomic, Molecular and Optical Physics*, 47(23), 2014.

[15] L Tonks and I Langmuir. Oscillations in ionized gases. *Physical Review*, 33(2):195 – 210, 1929.

[16] A. Modena, Z. Najmudin, A.E. Dangor, and et al. Electron acceleration from the breaking of relativistic plasma waves. *Nature*, 377(6550):606 – 608, 1995.

[17] F Albert and A Thomas. Applications of laser wakefield accelerator-based light sources. *Plasma Physics and Controlled Fusion*, 58(10):103001, sep 2016.

[18] R Egerton. *Physical Principles of Electron Microscopy*. Springer, 2005. P. 11, ISBN: 0-387-25800-0.

[19] T.D. Arber, K. Bennett, C.S. Brady, and et al. Contemporary particle-in-cell approach to laser-plasma modelling. *Plasma Physics and Controlled Fusion*, 57(11), 2015.

[20] S.S. Cerri, L. Franci, F. Califano, and et al. Plasma turbulence at ion scales: a comparison between particle in cell and eulerian hybrid-kinetic approaches. *Journal of Plasma Physics*, 83(2), 2017.

[21] M. Scheepers. Virtualization and containerization of application infrastructure : A comparison. *University of Twente*, 2014.

[22] C. Brady, K. Bennett, H. Schmitz, and C. Ridgers. *EPOCH User Manual*. University of Warwick, 2014.

[23] Central Laser Facility. Vulcan 20-20 upgrade. https://www.clf.stfc.ac.uk/Pages/Vulcan-2020.aspx. [Online; accessed 24-April-2024].

[24] J. Faure. Plasma injection schemes for laser-plasma accelerators. *CAS-CERN Accelerator School: Plasma Wake Acceleration 2014, Proceedings*, page 143 – 157, 2014.

[25] A. Gonsalves, K. Nakamura, C. Lin, and et al. Tunable laser plasma accelerator based on longitudinal density tailoring. *Nature Physics*, 7:862–866, 2011.

[26] P. Muggli. Beam-driven, plasma-based particle accelerators. 2016. Vol 1 (2016): Proceedings of the 2014 CAS-CERN Accelerator School: Plasma Wake Acceleration.

[27] J.P. Palastro, J.L. Shaw, P. Franke, and et al. Dephasingless laser wakefield acceleration. *Physical Review Letters*, 124(13), 2020.

[28] J.D. Sadler, C Arran, H Li, and et al. Overcoming the dephasing limit in multiple-pulse laser wakefield acceleration. *Phys. Rev. Accel. Beams*, 23:021303, 2020.

[29] J. P. Palastro, B. Malaca, J. Vieira, and et al. Laser-plasma acceleration beyond wave breaking. *Physics of Plasmas*, 28(1):013109, 01 2021.

[30] L. Whitmore, R.I. Mackay, M. van Herk, and et al. Focused vhee (very high energy electron) beams and dose delivery for radiotherapy applications. *Sci Rep*, 11:14013, 2011.

[31] EKSPLA. Ultraflux HE Series. https://ekspla.com/product/ultraflux-he-series-high-energy-femtosecond-opcpa-systems/specifications [Online; accessed 05-May-2024].